Na incorporation into Cu(In,Ga)Se₂ thin-film solar cell absorbers deposited on polyimide: Impact on the chemical and electronic surface structure

X. Song,[1] R. Caballero,[1,2] R. Félix,[1] D. Gerlach,[1] C. A. Kaufmann,[1] H.-W. Schock,[1] R. G. Wilks,[1] and M. Bär[1,3,a)]

[1]*Solar Energy Research, Helmholtz-Zentrum Berlin für Materialien und Energie GmbH, Lise-Meitner-Campus, Hahn-Meitner-Platz 1, 14109 Berlin, Germany*
[2]*Universidad Autónoma de Madrid, Departamento de Física Aplicada, C/Francisco Tomás y Valiente 7, 28049 Madrid, Spain*
[3]*Institut für Physik und Chemie, Brandenburgische Technische Universität Cottbus, Konrad-Wachsmann-Allee 1, 03046 Cottbus, Germany*

Na has deliberately been incorporated into Cu(In,Ga)Se₂ ("CIGSe") chalcopyrite thin-film solar cell absorbers deposited on Mo-coated polyimide flexible substrates by adding differently thick layers of NaF in-between CIGSe absorber and Mo back contact. The impact of Na on the chemical and electronic surface structure of CIGSe absorbers with various Cu-contents deposited at comparatively low temperature (420 °C) has been studied using x-ray photoelectron and x-ray excited Auger electron spectroscopy. We observe a higher Na surface content for the Cu-richer CIGSe samples and can distinguish between two different chemical Na environments, best described as selenide-like and oxidized Na species, respectively. Furthermore, we find a Cu-poor surface composition of the CIGSe samples independent of Na content and — for very high Na contents — indications for the formation of a (Cu,Na)–(In,Ga)–Se like compound. With increasing Na surface content, also a shift of the photoemission lines to lower binding energies could be identified, which we interpret as a reduction of the downward band bending toward the CIGSe surface explained by the Na-induced elimination of In$_{Cu}$ defects. © *2012 American Institute of Physics.* [doi:10.1063/1.3679604]

I. INTRODUCTION

Solar cells based on chalcopyrite thin-films on rigid glass substrates are heading for industrial maturity; Cu(In,Ga)Se₂ ("CIGSe") devices prepared on flexible substrates, however, are still mainly in the research and development stages. In addition to a reduced weight associated with replacing the glass substrates, flexible solar cells are expected to be produced at substantially lower production costs due to the application of cheaper substrate materials than the conventionally used soda-lime glass and by employing roll-to-roll deposition processes with very high through-put.[1] Flexible polyimide ("PI") is such a candidate substrate material for roll-to-roll processing of monolithically connected solar modules. Recently, the efficiency of CIGSe/Mo/PI-based solar cells could be improved to 18.7%.[2] The small efficiency difference compared to the highest CIGSe-based devices on rigid glass substrates ($\eta > 20\%$,[3]) can be explained by the process temperature which needs to be well below 500 °C when PI is used as a substrate.[4] In comparison high-efficiency devices on soda-lime glass substrates are typically obtained using growth temperatures of ∼550 °C. Furthermore, it is well known that in a conventional soda-lime glass substrate based CIGSe solar cell structure, Na from the soda-lime glass substrate diffuses into the absorber layer due to the elevated temperature during CIGSe

formation.[5–8] Na incorporation into the CIGSe absorber results in a significant improvement of solar cell efficiency,[9–12] and so for devices based on alternative (i.e., Na-free) substrates, Na must be added deliberately as part of the solar cell manufacturing process. Na can be incorporated prior to,[13,14] during,[12,15] or after[2,16] CIGSe growth. (Note that the latter approach requires a subsequent annealing process.)[15] Most commonly, Na binary compounds such as NaF, Na₂S, and Na₂Se[15] as well as NaCl[17] are employed as Na sources. The many diverse effects ascribed to the incorporation of Na in the CIGSe material have been summarized and discussed extensively.[18–22] While making no claim of being complete, the most prominent Na-related effects discussed in the past are:

1. Na (from the soda-lime glass substrate) is reported to diffuse through the Mo back contact layer at temperatures as low as 200 °C.[23]
2. Na accumulates at the CIGSe/Mo interface,[16,24] the surface (in the surface-near region) of the CIGSe absorber,[6,24] and the grain boundaries.[25,26] After removing Na from the CIGSe surface by means of, e.g. Ar⁺ ion sputtering[6] or wet chemical treatments,[27,28] it is reported that [while stored at room temperature under ultrahigh vacuum (UHV) conditions] Na reappears again at the CIGSe surface within days.[6]
3. Na affects the reaction mechanism of absorber formation[29–31] and hence the grain size, morphology, and texture of the CIGSe layer.[5,15,32,33]

a)Author to whom correspondence should be addressed. Electronic mail: marcus.baer@helmholtz-berlin.de.

4. Na increases the effective acceptor concentration in the CIGSe absorber by formation of antisite Na_{In} acceptor defects (Na on In site)[34] and/or by elimination of the compensating antisite In_{Cu} donor defect (In on Cu site)[13] and/or by neutralization of donor-like Se vacancies (V_{Se}) through Na-induced enhancement of oxygen chemisorption.[18,35]

5. If Na is available in stoichiometric quantities, it is proposed that Na replaces Cu and forms $NaInSe_2$[20,36] and/or (Cu,Na)–(In,Ga)–Se like compounds.[37,38]

Although taken into account on an empiric level in the CIGSe solar cell optimization and despite a full body of literature on how Na might modify the properties of the CIGSe thin-film solar cell absorbers (see above), it is still not clear which effect is the most crucial in terms of device performance. This paper hence focuses on the open questions about the mechanism behind the beneficial effects of Na incorporation when flexible substrates and low deposition temperatures are employed. In particular, the influence of Na (deliberately introduced as NaF before CIGSe deposition) on the chemical and electronic surface structure of CIGSe thin-film solar cell absorbers deposited on flexible PI substrates is studied by x-ray photoelectron (XPS) and x-ray excited Auger electron (XAES) spectroscopy.

II. EXPERIMENT

Commercially available PI foil (UBE Upilex 25S) was used as the flexible substrate (5×5 cm^2 in size). As the back contact a Mo layer (800 nm) was deposited by dc-sputtering. The CIGSe absorber layer was grown on the Mo-coated PI foils using a multistage coevaporation process.[14] Before starting the deposition process, the substrates were exposed to Se for 6 min at a nominal temperature of 330 °C. During the first stage of the deposition process the substrate temperature was maintained at 330 °C. During the second and third stages, the nominal substrate temperature was increased to 420 °C, as measured by a reference thermocouple placed between the heater and the rear side of the processed sample. Two sample series were prepared for our investigation. Both series were intentionally deposited Cu-poor with respect to the standard Cu:(In + Ga):Se = 1:1:2 CIGSe stoichiometry, but the degree of Cu deficiency was varied by adjusting the duration of the third deposition stage.[39] It should be noted, however, that the nominal Cu/(In + Ga) composition at the end of second deposition stage was approx. 1.15. For convenience, in this manuscript we will refer to the two sample series in terms of their *relative* Cu content as "Cu-rich" and "Cu-poor." In order to deliberately add Na to the absorber, a NaF precursor was evaporated onto the Mo-coated PI substrate prior to the deposition of the CIGSe thin films. Each CIGSe series consisted of four samples with different NaF precursor thickness. The nominal thicknesses of the NaF precursors are 0 (Na-free samples), 8, 16, and 32 nm. In addition, CIGSe reference samples for the Cu-rich and Cu-poor process deposited on soda-lime glass were prepared for bulk composition and thickness measurements performed by x-ray fluorescence analysis (XRF) using a Philips MagiXPro PW 2400 spectrometer. The results are shown in Table I.

TABLE I. Bulk composition and thickness of CIGSe reference samples deposited on soda-lime glass [(III: In+Ga; experimental uncertainty: $\pm0.05\%$ (composition) and $\pm0.05\,\mu$m (thickness)] as measured by x-ray fluorescence.

Referred series	Cu (%)	In (%)	Ga (%)	Se (%)	Cu/III	Ga/III	Thickness (μm)
Cu-rich	22.26	21.70	5.30	50.74	0.82	0.20	1.38
Cu-poor	16.23	23.61	7.44	52.72	0.52	0.24	1.49

Note that based on our previous Na-content optimization experiments on CIGSe absorbers having a similar composition than the here-considered "Cu-rich" samples,[14] one would expect the highest power conversion efficiencies from solar cell devices based on the 16 nm NaF CIGSe absorbers.

In order to avoid air exposure of the prepared CIGSe/Mo/PI samples, they were taken out of the absorber deposition chamber using a N$_2$-filled glovebag and transferred to a N$_2$-purged glovebox. To minimize contamination the samples were additionally stored in an UHV storage chamber inside the glovebox before XPS/XAES measurements. For these measurements, the samples were cut into 2.0×1.3 cm^2 pieces, mounted on glass plates for support, and finally transferred from the glovebox into the attached UHV (base pressure: 3×10^{-9} mbar) surface analysis system. An Mg K$_\alpha$ (1253.56 eV) and Al K$_\alpha$(1486.58 eV) twin anode x-ray source (SPECS XR 50) was used for excitation. A SPECS PHOIBOS 150 MCD-9 hemispherical electron analyzer (calibrated according to Ref. 40) was employed for electron detection. For each sample a survey spectrum was first obtained to identify the elements present in the absorber surface before narrower detail scans of selected peaks were measured. Note that the information depth of the XPS/XAES measurements is limited by the inelastic mean free path (IMFP) of the electrons, which depends on the material and the excitation energy and ranges from approx. 0.5–4 nm (Ref. 41) in the current study. For electrons of the intensity I_0 emitted at a depth d below the sample surface, the intensity at the surface I is attenuated according to $I_0 \times e^{-d/IMFP}$; thus while the XRF measurements can be considered to probe the sample *bulk*, the XPS/XAES measurements exclusively probe the topmost *surface* of the sample.

III. RESULTS AND DISCUSSION

A. Survey spectra

The Mg K$_\alpha$ XPS survey spectra (normalized to the background at a binding energy, E_{bin}, of 870.6 eV) of the Cu-rich and Cu-poor sample series are displayed in Fig. 1. The most prominent photoemission and Auger lines can be ascribed to the CIGSe absorber elements (Cu, In, Ga, and Se). Furthermore, low-intensity C- and O-related signals can be observed in the spectra. Na 1s photoemission lines (the most prominent Na-related XPS/XAES feature at E_{bin} = 1071 eV) can clearly be identified in the survey spectra of the Cu-rich samples which were prepared with 16 and 32 nm NaF. For the Cu-poor samples the respective Na 1s peaks appear smaller but can also be observed for the 16 and 32 nm NaF sample.

Na has apparently diffused from the CIGSe/Mo back contact through the CIGSe absorber layer to the surface of
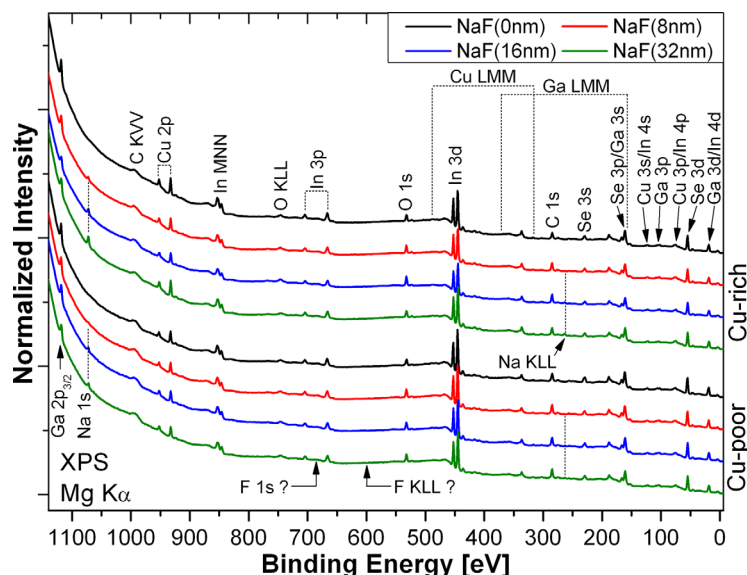
FIG. 1. (Color online) Mg K$_\alpha$ XPS survey spectra of the Cu-rich (top four spectra) and Cu-poor (bottom four spectra) CIGSe sample series. The employed NaF precursor thickness is indicated by the following color code: 0 nm (black), 8 nm (red), 16 nm (blue), 32 nm (green).

these samples. Interestingly, in the spectral regions where one would expect the most prominent F-related photoemission (F 1s at $E_{bin} = 685$ eV) and Auger (F $KL_{23}L_{23}$ at $E_{bin} = 599$ eV) line, no signals can be observed — even the F KLL detail spectra (not shown) do not show any indication of fluorine being present at the samples surface. Note that we do observe F in compositional depth profiles (determined from secondary ion-mass spectroscopy measurements, not shown) of similarly prepared samples at a much lower concentration than Na and primarily located in the absorber bulk close to the CIGSe/Mo interface. Hence, fluorine apparently does not diffuse through the CIGSe during absorber formation to the surface but rather remains at the absorber/back contact interface.

B. XPS and XAES detail spectra of Na

In order to study the Na surface content and how it changes with increasing NaF precursor layer thickness, the detail spectra of the Na 1s photoemission and the Na $KL_{23}L_{23}$ Auger lines of the two sample sets were recorded.

The respective spectra are shown (normalized to the background at $E_{bin} = 1076$ eV and to that at a kinetic energy, E_{kin}, of 985.5 eV, respectively) in Fig. 2. For all samples with a NaF precursor layer, Na 1s and Na KLL signals can be observed. As expected, the Na signal intensity increases in accordance with the thickness of the employed NaF layer. Comparing the intensity of the Na-related signals of the two sample series, one can observe that those of the Cu-rich CIGSe absorbers are always higher than those of the Cu-poor samples, which points to a different incorporation/diffusion mechanism.

Elemental depth profiles based on glow discharge optical emission spectrometry (GDOES) measurements on similarly-prepared Cu-poor and Cu-rich CIGSe samples on soda-lime glass substrates indeed show that while one finds a significant amount of Na only at the surface of the absorber and its interface to the Mo/glass substrate for the Cu-rich CIGSe sample, for the respective Cu-poor CIGSe a significant Na content can also be detected throughout the entire absorber bulk.[39] At first, this seems to be in contradiction to our finding of a higher Na content at the surface of the
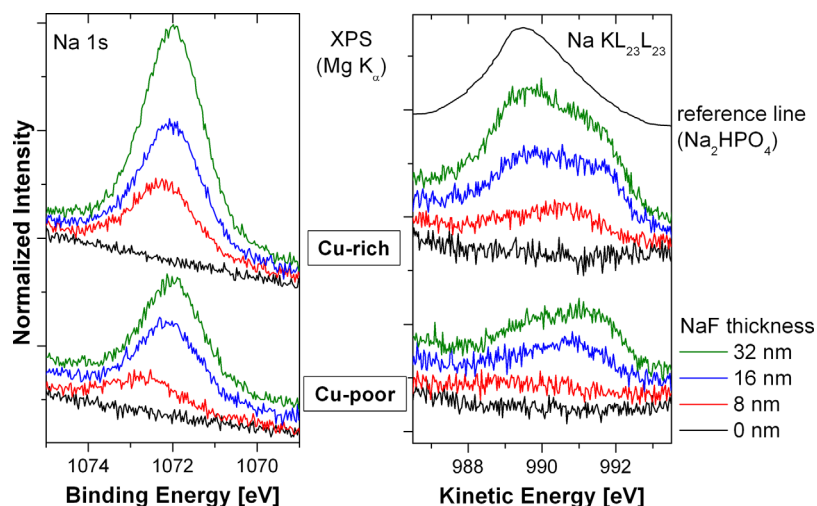

FIG. 2. (Color online) Mg K$_\alpha$ detail spectra of the Na 1s photoemission (left) and the Na $KL_{23}L_{23}$ Auger line (right) of the investigated samples of the Cu-rich and Cu-poor sample series, normalized to the background. For comparison, the reference Na $KL_{23}L_{23}$ XAES spectrum of Na$_2$HPO$_4$ is also shown (digitized from Ref. 42).

Cu-rich compared to that of the Cu-poor CIGSe/Mo/PI samples. This discrepancy can be explained taking into account that according to Wei *et al.*[20] the main effect of Na (present in small quantities) is the elimination of In_{Cu} defects, which preferably form in Cu-poor CIGSe absorbers. If the CIGSe material is grown with a limited Na supply — as in the case of adding Na precursors when using Na-free substrates (in contrast to using soda-lime glass substrates which can be considered as infinite Na source) — less Na is used up to eliminate In_{Cu} sites in the bulk of a Cu-rich compared to a Cu-poor absorber. Hence, given equal initial Na quantities, more Na will accumulate at the CIGSe surface when preparing Cu-rich compared to Cu-poor CIGSe material.

C. Na speciation

Comparing the Na $KL_{23}L_{23}$ Auger line of a single Na reference species (as, e.g., Na_2HPO_4, digitized from Ref. [42]) with the Na *KLL* spectra of the investigated CIGSe samples (Fig. 2, right panel), it can be concluded that the measured Na Auger lines are composed of contributions from (at least) two different Na species. In order to identify the Na species formed, the modified Auger parameter $[\alpha^*(Na) = E_{bin}(Na\ 1s) + E_{kin}(Na\ KLL)]$ was determined. For that the individual Na *KLL* positions have been estimated by fitting the Na *KLL* line by two Voigt functions (for the two different Na species). Besides an energetic shift and comparatively broad peaks, we do not find as clear an indication for more than one species in the case of the Na 1s line, due to very similar $E_{bin}(Na\ 1s)$ for the different Na species in question.[43] Thus to compute $\alpha^*(Na)$, we use only one Na 1s position, which was determined by a simultaneous fit of the data using Voigt profiles with coupled Gaussian and Lorentzian widths and including a linear background. The resulting $\alpha^*(Na)$ are compared to literature values[6,29,42,43] for different Na reference compounds in Fig. 3. Note that for the literature values, either the reported range is given or the same uncertainty as in our measurements was assumed. The computed $\alpha^*(Na)$

values form two groups, confirming our earlier conclusion that (at least) two different Na species would be present at the CIGSe sample surfaces. The $\alpha^*(Na)$ values of "species (1)" ["species (2)"], we find between 2062.8 and 2063.3 eV [2061.0 and 2061.6 eV] (± 0.2 eV). First, we can exclude a contribution of metallic Na [$\alpha^*(Na) = 2065.4...$ 2066.3 eV,[6,43]] or NaF. Although in the latter case, $\alpha^*(Na)$ of species (2) agrees with the upper limit of the reported $\alpha^*(Na)$ values of NaF, we can exclude this contribution due to the absence of any F-derived XPS/XAES signal (see discussion above). The comparison with the reported $\alpha^*(Na)$ values shown in Fig. 3 reveals that while $\alpha^*(Na)$ of species (1) is similar to that of Na_2Se_X, $\alpha^*(Na)$ of species (2) is in the same energy region as the $\alpha^*(Na)$ values of Na_2O, Na_2SeO_3, and Na_2CO_3. However, because the main contribution to the O 1s line of these CIGSe samples is found at a E_{bin}— approximately 2.5 eV higher than what one would expect for the O 1s XPS line of Na_2O (529.7 eV[43]) — a significant contribution of Na_2O can also be excluded. Thus, species (1) can presumably best be described as Na in a selenide environment, while species (2) represents Na in an oxidized environment. With reference to the results of Heske *et al.*,[6] we hence could call species (1) "unreacted" and species (2) "reacted," which is also confirmed by the corresponding $\alpha^*(Na)$ values (Fig. 3). Note that according to Heske *et al.*,[6] the "unreacted" Na species is characterized by a binding character intermediate between metallic and ionic Na, while the "reacted" Na species coexists with SeO_2 and is characterized by chemical inactivity.

D. Surface composition

In order to investigate the chemical surface composition of the investigated samples (and how it changes upon NaF addition), the XPS line intensities were quantified by simultaneous fits of all respective spectra by Voigt profiles including a linear background. The intensities of the most prominent Ga $2p_{3/2}$, Cu $2p_{3/2}$, In $3d_{3/2}$, and Se 3s XPS lines — normalized to the corresponding intensities of the Na-free ("0 nm") sample—are shown in Fig. 4. One can observe that for both sets of samples the CIGSe-related peak intensities primarily decrease with increasing Na precursor layer thickness. This intensity reduction can be ascribed to the attenuation of the CIGSe-related XPS peaks related to Na accumulation at the sample surface (i.e., an increasing
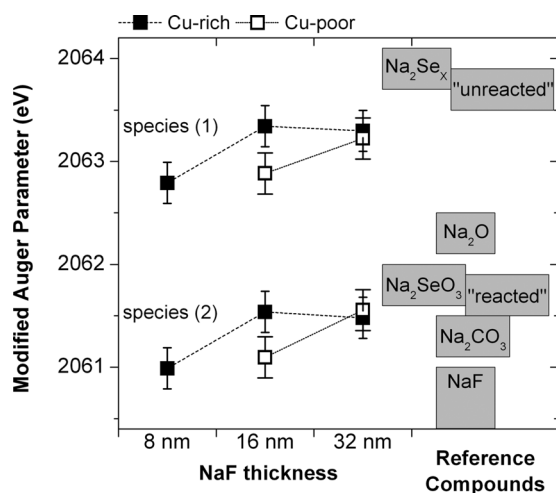
FIG. 3. Modified Na Auger parameters of the two Na species (1) and (2) derived from XPS/XAES measurements of the Cu-rich and Cu-poor CIGSe samples. The boxes indicate literature values of modified Auger parameters of Na reference compounds taken from Refs. 6, 29, 42, and 43.
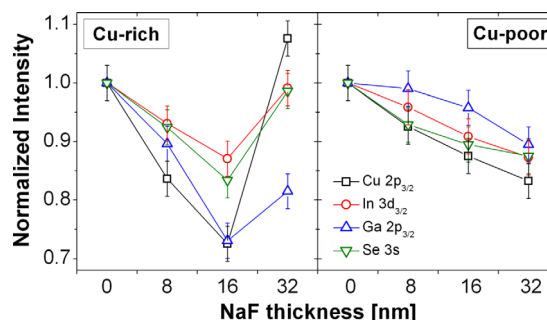
FIG. 4. (Color online) Normalized intensities of the probed photoemission lines for the Cu-rich (left) and Cu-poor (right) CIGSe samples as a function of increasing NaF precursor layer thickness.

thickness of the formed Na surface species). Hence, the less-pronounced decrease of the peak intensities observed for the Cu-poor CIGSe samples is due to the observed lower Na surface content (see Fig. 2 and discussion above). Interestingly, for the Cu-rich CIGSe sample with a NaF precursor layer of 32 nm thickness, the CIGSe-related (in particular the Cu $2p_{3/2}$) photoemission line intensities are significantly increased. This hints at a potential incorporation of Na into the lattice of the upper CIGSe region rather than the mere accumulation of Na at the sample surface. This hypothesis will be further elaborated in conjunction with the consideration of the determined surface composition that follows.

The surface compositions of both Cu-rich and Cu-poor samples are calculated on the basis of the quantified Ga $2p_{3/2}$, Cu $2p_{3/2}$, In $3d_{3/2}$, Se $3s$, and Na $1s$ XPS line intensities, after correcting for the corresponding photoionization cross section,[44] the inelastic mean free path,[41] and the transmission function of the electron analyzer.[45] The surface composition determined for the Cu-rich and -poor samples as a function of the NaF precursor layer thickness is shown in Fig. 5. Note that while Fig. 5(a) presents the relative surface composition neglecting a potential Na contribution, Fig. 5(b) shows the composition taking Na into account. Compared to the XRF-derived *bulk* composition presented in Table I and shown in Fig. 5(a), we find a Cu-poor *surface* composition for all samples (mostly independent of the Na content). More specifically, the bulk composition of the Cu-rich (Cu-poor) CIGSe sample is in fair agreement with (significantly deviates from) the Cu:(In + Ga):Se = 1:1:2 stoichiometry (as indicated in Fig. 5). At the same time — independent of bulk composition — we find a very similar surface composition for both sets of samples, which is (within the error bars) in reasonable agreement with a Cu:(In + Ga):Se = 1:3:5 composition. This Cu-poor surface composition is well-known for high-efficiency Cu-poor processed CIGSe samples.[46–48]

The potential impact of the presence of Na on the chemical surface structure is shown in Fig. 5(b). As expected, it can be observed that the relative Na content increases with NaF precursor layer thickness. Interestingly, the Na content approaches (exceeds) that of Cu for the 32 nm NaF Cu-poor (Cu-rich) samples.

Together with the observed increase of the absorber elements for the 32 nm NaF Cu-rich CIGSe sample discussed in conjunction with Fig. 4, this might indicate that at these high Na contents it becomes necessary to also consider that Na could be incorporated in the chalcopyrite lattice and does not only accumulate on the CIGSe absorber in form of surface species. In this context, we note that Stanbery *et al.*[37] and later also Nadenau *et al.*[38] suggested the formation of Na-containing CIGSe phases, such as $Cu_2Na_3In_5Se_{10}$ or Cu_2Na_3-Ga_5Se_{10}, in the Na-Cu-In-Se or Na-Cu-Ga-Se system, respectively. In our case the direct comparison of the corresponding Cu:Na:(In+Ga):Se stoichiometry of 2:3:5:10 [see Fig. 5(b)] with the Na and Cu content of the 32 nm NaF Cu-rich CIGSe sample reveals a rather good agreement. The small deviation of the experimentally derived Se and (In + Ga) data from the nominal 2:3:5:10 composition, however, indicates that the chemical surface structure of CIGSe thin-film solar cell absorbers with high Na contents is more complicated. Instead of a simple $Cu_2Na_3(In,Ga)_5Se_{10}$/CIGSe bi-layer system, the Na-rich CIGSe surface structure is most likely a mixture of a variety of different (spatially isolated?) phases including Na binaries (see section C), Cu-poor chalcopyrites (see this section, above), and (Cu,Na)–(In,Ga)–Se-like compounds. The presence of the latter is not in contradiction to the Na compound speciation above, since α^*(Na) of a $Cu_2Na_3(In,Ga)_5Se_{10}$-like species is expected to be in the same energetic regime as that of the "unreacted" selenide Na species (1). Please also note that the formation of Cu-free $NaInSe_2$-like compounds at the CIGSe surface in the high Na-content regime as suggested by Refs. 20 and 36 cannot be brought in-line with our observation of significantly increased Cu-related photoemission line intensities for the 32 nm NaF Cu-rich CIGSe sample (see Fig. 4).
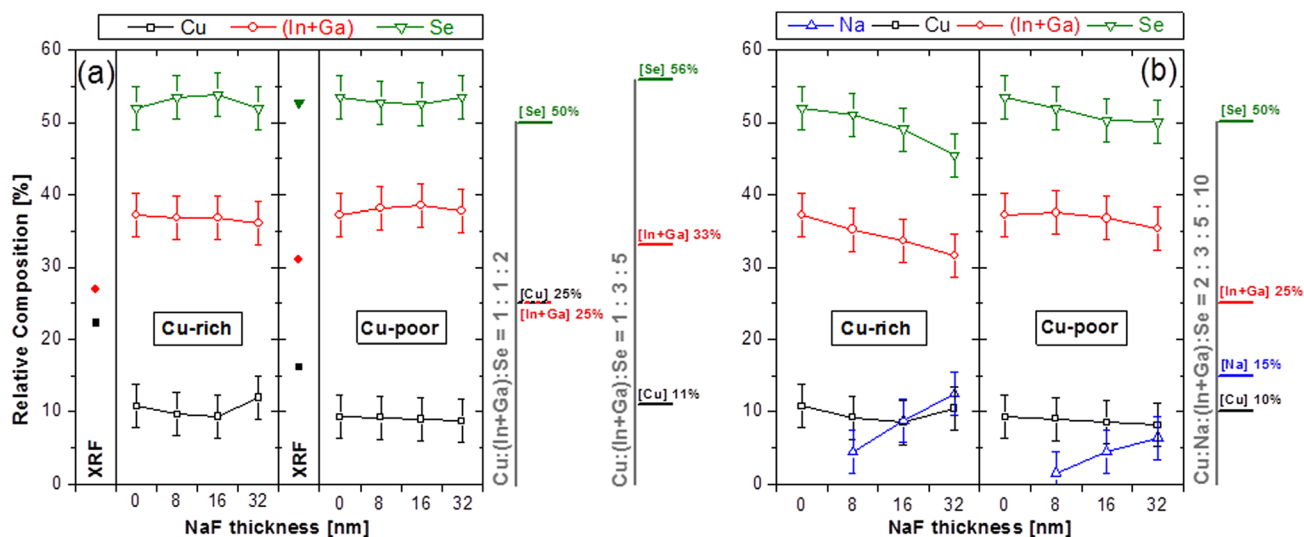

FIG. 5. (Color online) Relative surface composition for the Cu-rich and Cu-poor CIGSe samples as a function of the NaF precursor layer thickness excluding (a) and including (b) the Na content. In (a) the bulk composition (as derived by XRF) of a respective CIGSe absorber deposited on soda-lime glass is also shown. The horizontal lines indicate the nominal stoichiometries of a Cu:(In + Ga):Se = 1:1:2 and 1:3:5 phase, as well as that of a Cu:Na:(In + Ga):Se = 2:3:5:10 compound.

E. Binding energy shift

As part of the photoemission line fitting for quantification, the binding energies were also determined. Plotting the E_{bin} values of various photoemission lines as function of the NaF precursor layer thickness with respect to the initial value (i.e., NaF thickness = 0 nm; see Fig. 6), a pronounced negative E_{bin} shift can be observed. This shift is associated with a decrease in E_{bin} and hence with increasing NaF thickness, we find an upward band bending with respect to the Fermi energy. Our finding is in contrast to the results of Heske *et al.*[6,49] and Klein *et al.*,[50] who report a E_{bin} increase and, consequently, a downward band bending with increasing Na content on the CIGSe surface. One explanation for this variance could be the differing natures of the Na supplies. While in our case the Na (provided as NaF precursor layer) diffuses through the CIGSe absorber layer forming a very complex chemical surface structure (see discussion in section D), the experiments of Heske *et al.*[6,49] and Klein *et al.*[50] are based on the *in situ* deposition of (metallic) Na on sputter-cleaned CIGSe samples and UHV-cleaved $CuInSe_2$ single crystals, respectively.

The upward band bending with increasing Na surface content observed here can be understood as follows: A Cu-poor 1:3:5-like surface composition (which we observe for the samples of the Cu-rich and Cu-poor CIGSe series, see Sec. D) was explained in the past by the formation of an ordered defect compound (ODC) layer[46,47] or by surface reconstruction.[51,52] While according to first-principles calculations the ODC can be considered as periodic repetition of the charge compensated ($2 V_{Cu}^{-} + In_{Cu}^{2+}$) defect complex (as described in Ref. 53), it was also suggested by theory that the surface reconstruction is based on the formation of the energetically most favorable metal-terminated (112) and selenium-terminated ($1\bar{1}2$) CIGSe surfaces stabilized through V_{Cu}^{-} and subsurface In_{Cu}^{2+} defects, respectively.[54,55] In either case, the large defect population in chalcopyrites plays a crucial role for the explanation of the Cu-poor surface. As already mentioned above, theory also predicts that the main effect of sodium in the CIGSe material is the elimination of In_{Cu}^{2+} defects by replacing In on nominal Cu sites ($\rightarrow Na_{Cu}$).[20] As a consequence, the total amount of positive charges close to the CIGSe surface and the related

downward band bending toward the CIGSe surface (repeatedly indicated by photoemission experiments, as the Fermi energy is closer to conduction band minimum than to the valence band maximum[56–58]) would be reduced. This reduction of the *downward* band bending could also be interpreted as a relative *upward* band bending, and so this reasoning is consistent with our photoemission data. Note that while the E_{bin} shift within one sample series (i.e., for the Cu-poor or Cu-rich CIGSe samples) is very similar, the spread as well as the shift of the binding energies for the Cu-poor samples appears to be slightly larger. Following the above explanation, the latter can be understood by taking the initial downward surface band bending into account, which can legitimately be assumed to be more pronounced for the Cu-poor CIGSe samples.

Downward band bending toward the CIGSe surface is considered to be a prerequisite for high-efficiency devices,[59] and so the finding that with increasing Na content the downward surface band bending is reduced might offer an explanation why Na becomes detrimental for the device performance when its concentration is too high.[60,61]

IV. SUMMARY AND CONCLUSION

The present study addresses the influence of Na on the chemical and electronic structure of CIGSe thin-film solar cell absorbers with different levels of Cu-deficiency deposited on Mo-coated polyimide flexible substrates at comparatively low process temperatures (420 °C instead of around 550 °C—the standard deposition temperature when using rigid soda-lime glass substrates). The Na content was deliberately tuned by employing different thicknesses (0–32 nm) of NaF precursor layers on the Mo/PI substrates before CIGSe deposition.

We find that CIGSe-related photoemission line intensities primarily decrease with increasing NaF precursor thickness, which is explained by an increasingly-pronounced accumulation of Na on the CIGSe absorber (in the form of surface species). A higher Na surface content is found for the (relatively) Cu-rich CIGSe layers. This effect was attributed to the elimination of In_{Cu} sites[20] — which are expected to be present in a given CIGSe material in a concentration proportional to its degree of Cu-deficiency — by Na and to the limited supply of Na available to do so. At least two different Na species could be identified on the investigated sample surfaces. Species (1) could best be described as Na in a selenide environment, while species (2) represents Na in an oxidized environment. In agreement with the results of Heske *et al.*,[6] species (1) could also be called "unreacted" and species (2) "reacted." The comparison of the bulk and surface compositions revealed that while the bulk of the relatively Cu-rich (Cu-poor) CIGSe samples is in agreement with (deviates from) the nominal Cu:(In,Ga):Se = 1:1:2 stoichiometry, the surface composition of all samples (independent of bulk composition or Na surface content) is in accordance with a 1:3:5 stoichiometry. Besides this general behavior, for the highest Na-contents we also find clear indications for the formation of a (Cu,Na)–(In,Ga)–Se-like compound, such as $Cu_2Na_3(In,Ga)_5Se_{10}$. Furthermore, the CIGSe photoemission
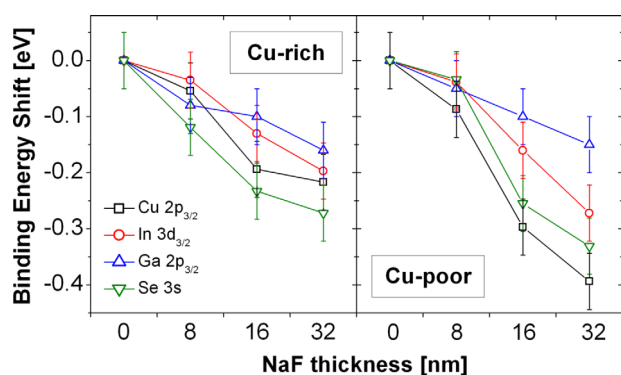

FIG. 6. (Color online) Binding energy shifts of the probed photoemission lines for the Cu-rich (left) and Cu-poor (right) CIGSe samples as a function of increasing NaF precursor layer thickness.

lines can be observed to shift to lower binding energy with increasing Na surface content. The related relative upward band bending was interpreted as a reduction of the downward band bending toward the CIGSe surface, explained by a reduction of the positive charges in the CIGSe surface region when Na eliminates In_{Cu} sites.[20]

These findings demonstrate how strongly the chemical and electronic surface structure of CIGSe thin-film solar cell absorbers is affected by different Na contents. Thus the optimization of the Na concentration in the CIGSe material needs special attention, particularly if one uses alternative (i.e., Na-free) substrates. The observation that the Na-induced effects not only depend on the Na content but also on the degree of the CIGSe Cu-deficiency reveals that the interaction of Na with the significant defect population in CIGSe seems to dominate the impact of Na on the chemical and electronic properties and hence is most likely the key to understanding the (beneficial) Na effect in the chalcopyrite material class. Experiments on how the deposition of the *pn*-junction partner CdS using the commonly employed chemical bath deposition changes the chemical and electronic structure of the different CIGSe surfaces (then buffer/absorber interfaces) are currently ongoing.

ACKNOWLEDGMENTS

[1] K. Otte, L. Makhova, A. Braun, and I. Konovalov, Thin Solid Films **511–512**, 613 (2006).

[2] A. Chirilâ, P. Blösch, S. Seyrling, A. Uhl, S. Buecheler, F. Pianezzi, C. Fella, J. Perrenoud, L. Kranz, R. Verma, D. Guettler, S. Nishiwaki, Y. E. Romanyuk, G. Bilger, D. Brémaud, and A. N. Tiwari, Prog. Photovoltaics **19**, 560 (2011); A. Chirilâ, S. Buecheler, F. Pianezzi, P. Blösch, Ch. Gretener, A. R. Uhl, C. Fella, L. Kranz, J. Perrenoud, S. Seyrling, R. Verma, S. Nishiwaki, Y. E. Romanyuk, G. Bilger, A. N. Tiwari, Nature Mater. **10**, 857 (2011).

[3] P. Jackson, D. Hariskos, E. Lotter, S. Paetel, R. Wuerz, R. Menner, W. Wischmann, and M. Powalla, Prog. Photovoltaics **19**, 894 (2011).

[4] D. Bremaud, D. Rudmann, G. Bilger, H. Zogg, and A. N. Tiwari, *Proc. 31st IEEE Photovoltaic Specialist Conference*, Lake Buena Vista, FL (IEEE, Piscataway, NJ 2005), pp. 223–226.

[5] M. Bodegard, L. Stolt, and J. Hedstrom, *Proc. 12th European Solar Energy Conference*, Amsterdam, The Netherlands (HS Stephens, Bedford, UK, 1994), pp. 1743–1746.

[6] C. Heske, R. Fink, E. Umbach, W. Riedl, and F. Karg, Appl. Phys. Lett. **68**, 3431 (1996).

[7] A. Rockett, K. Granath, S. Asher, M. M. Al Jassim, F. Hasoon, R. Matson, B. Basol, V. Kapur, J. S. Britt, T. Gillespie, and C. Marshall, Sol. Energy Mater. Sol. Cells **59**, 255 (1999).

[8] M. B. Zellner, R. W. Birkmire, E. Eser, W. N. Shafarman, and J. G. Chen, Prog. Photovoltaics **11**, 543 (2003).

[9] V. Probst, J. Rimmasch, W. Riedl, W. Stetter, J. Holz, H. Harms, F. Karg, and H. W. Schock, *Proc. 1st World Conference on Photovoltaic Energy Conversion*, Waikoloa, Hawaii, 1994 (IEEE, New York, 1995), p. 144.

[10] J. E. Granata, J. R. Sites, S. Asher, and R. J. Matson, *Proc 26th IEEE Photovoltaic Specialists Conference* (1997), p. 387.

[11] R. W. Birkmire and E. Eser, Ann. Rev. Mater. Sci. **27**, 625 (1997).

[12] T. Watanabe, H. Nakazawa, and M. Matsui, Jpn. J. Appl. Phys. **37**, L1370 (1998).

[13] M. A. Contreras, B. Egaas, P. Dippo, J. Granata, K. Ramanathan, S. Asher, A. Swartzlander, and R. Noui, *Proc. 26th IEEE Photovoltaic Specialists Conference*, Anaheim, CA (IEEE, Piscataway, NJ 1997), p. 359.

[14] R. Caballero, C. A. Kaufmann, T. Eisenbarth, T. Unold, R. Klenk, and H. W. Schock, Prog. Photovoltaics **19**, 547 (2011).

[15] M. Bodegård, K. Granath and L. Stolt, Thin Solid Films **361–362**, 9 (2000) and references therein.

[16] D. Rudmann, A. F. da Cunha, M. Kaelin, F. Kurdesau, H. Zogg, A. N. Tiwari, and G. Bilger, Appl. Phys. Lett. **84**, 1129 (2004).

[17] A. N. Tiwari, M. Krejci, F.-J. Haug and H. Zogg, Prog. Photovoltaics **7**, 393 (1999).

[18] L. Kronik, D. Cahen, and H.-W. Schock, Adv. Mater. **10**, 31 (1998).

[19] U. Rau and H.-W. Schock, Appl. Phys. A: Mater. Sc. Process. **69**, 131 (1999).

[20] S.-H. Wei, S. B. Zhang, and A. Zunger, J. Appl. Phys. **85**, 7214 (1999).

[21] M. Kemell, M. Ritala, and M. Leskelä, Crit. Rev. Solid State Mater. Sci. **30**, 1 (2005).

[22] U. P. Singh and S. P. Patra, Int. J. Photoenergy **2010**, 468147 (2010).

[23] D. Schmid, M. Ruckh, and H.-W. Schock, Sol. Energy Mater. Sol. Cells **41–42**, 281 (1996).

[24] J. H. Scofield, S. Asher, D. Albin, J. Tuttle, M. Contreras, D. Niles, R. Reedy, A. Tennant, and R. Noufi, *Proc. 24th IEEE Photovoltaic Specialists Conference* (IEEE, New York, 1995), pp. 164–167.

[25] D. W. Niles, M. Al-Jassim, and K. Ramanathan, J. Vac. Sci. Technol. A **17**, 291 (1999).

[26] O. Cojocaru-Mirédin, P. Choi, R. Wuerz, and D. Raabe, Ultramicroscopy **111**, 552 (2011).

[27] A. Kylner, J. Electrochem. Soc. **146**, 1816 (1999).

[28] M. Bär, M. Rusu, S. Lehmann, S. Sokoll, A. Grimm, I. M. Kötschau, I. Lauermann, P. Pistor, L. Weinhardt, O. Fuchs, C. Heske, Ch. Jung, W. Gudat, Th. Schedel-Niedrig, M. C. Lux-Steiner, and Ch. -H. Fischer, *Proc. 31st IEEE Photovoltaic Specialists Conference*, Boca Raton, FL (IEEE, Piscataway, 2005), pp. 307–310.

[29] D. Braunger, D. Harsikas, G. Bilger, U. Rau, and H.-W. Schock, Thin Solid Films **361–362**, 161 (2000).

[30] F. Hergert, R. Hock, A. Weber, M. Purwins, J. Palm, and V. Probst, J. Phys. Chem. Solids **66**, 1903 (2005).

[31] F. Hergert, S. Jost, R. Hock, M. Purwins, and J. Palm, Thin Solid Films **515**, 5843 (2007).

[32] J. Hedström, H. Ohlsén, M. Bodegård, A. Kylner, L. Stolt, D. Hariskos, M. Ruckh, and H. W. Schock, *Proc. 23rd IEEE Photovoltaic Specialists Conference*, Louisville, KY (IEEE, Piscataway, NJ, 1993), p. 364.

[33] V. Probst, J. Rimmasch, W. Stetter, H. Harms, W. Riedl, J. Holz, and F. Karg, *Proc. 13th European Photovoltaic Solar Energy Conference*, Nice, France (HS Stephens, Bedford, UK, 1995), p. 2126.

[34] D. W. Niles, K. Ramanathan, F. Hasoon, R. Noufi, B. J. Tielsch, and J. E. Fulghum, J. Vac. Sci. Technol. A **15**, 3044 (1997).

[35] M. Ruckh, D. Schmid, M. Kaiser, R. Schaffler, T. Walter, and H.-W. Schock, *Proc. 1st World Conference on Photovoltaic Energy Conversion*, Waikoloa, Hawaii, 1994 (IEEE, New York, 1995), p. 156.

[36] K. Fukuzaki, S. Kohiki, H. Yoshikawa, S. Fukushima, T. Watanabe, and I. Kojima, Appl. Phys. Lett. **73**, 1385 (1998).

[37] B. J. Stanbery, C.-H. Chang, and T. J. Anderson, *Inst. Phys. Conf. Ser.* **152**, 915 (1997).

[38] V. Nadenau, G. Lippold, U. Rau, and H.-W. Schock, J. Cryst. Growth **233**, 13 (2001).

[39] R. Caballero, Ch. A. Kaufmann, V. Efimova, T. Rissom, V. Hoffmann, and H.-W. Schock, Prog. Photovoltaics, published online: 30 DEC 2011, DOI: 10.1002/pip.1233 (2011).

[40] D. Briggs and M. P. Seah, *Auger and X-Ray Photoelectron Spectroscopy: Practical Surface Analysis* (Wiley, New York, 1990), Vol. 1, Appendix 1.

[41] S. Tougaard, QUASES-IMP-TPP2M, Version 2.2, http://www.quases.com/; S. Tanuma, C. J. Powell, and D. R. Penn, Surf. Interface Anal. **21**, 165 (1993).

[42] J. Chastain, J. F. Moulder, W. F. Stickle, P. E. Sobol and K. D. Bomben, eds., *Handbook of X-ray Photoelectron Spectroscopy* (Perkin-Elmer, Minnesota, 1992).

[43] NIST X-ray Photoelectron Spectroscopy Database, Version 3.5 (National Institute of Standards and Technology, Gaithersburg, MD, 2003) http://srdata.nist.gov/xps/.

[44] J. H. Scofield, J. Electron Spectrosc. Relat. Phenom. **8**, 129 (1976).

[45] The transmission function was determined by normalizing a survey spectrum of a clean Ag foil so that it agreed with (the background of) an absolute reference Ag survey spectrum taken from M. P. Seah, G. C. Smith, Surf. Interface Anal. **15**, 751 (1990).

[46] J. R. Tuttle, D. S. Albin, and R. Noufi, Sol. Cells **30**, 21 (1991).

[47] D. Schmid, M. Ruckh, F. Grunwald, and H.-W. Schock, J. Appl. Phys. **73**, 2902 (1993).

[48] M. Bär, I. Repins, M. A. Contreras, L. Weinhardt, R. Noufi, and C. Heske, Appl. Phys. Lett. **95**, 052106 (2009).

[49] C. Heske, G. Richter, Z. Chen, R. Fink, E. Umbach, W. Riedl, and F. Karg, J. Appl. Phys. **82**, 2411 (1997).

[50] A. Klein, T. Löher, C. Pettenkofer, and W. Jaegermann, J. Appl. Phys. **80**, 5039 (1996).

[51] D. Liao and A. Rockett, Appl. Phys. Lett. **82**, 2829 (2003).

[52] H. Mönig, Ch.-H. Fischer, R. Caballero, Ch. A. Kaufmann, N. Allsop, M. Gorgoi, R. Klenk, H.-W. Schock, S. Lehmann, M. C. Lux-Steiner, and I. Lauermann, Acta Mater. **57**, 3645 (2009).

[53] S. B. Zhang, S.-H. Wei, A. Zunger, and H. Katayama-Yoshida, Phys. Rev. B **57**, 9642 (1998).

[54] S. B. Zhang and S.-H. Wei, Phys. Rev. B **65**, 081402(R) (2002).

[55] J. E. Jaffe and A. Zunger, Phys. Rev. B **64**, 241304(R) (2001).

[56] M. Morkel, L. Weinhardt, B. Lohmüller, C. Heske, E. Umbach, W. Riedl, S. Zweigart, and F. Karg, Appl. Phys. Lett. **79**, 4482 (2001).

[57] A. Klein and W. Jaegermann, Appl. Phys. Lett. **74**, 2283 (1999).

[58] M. Bär, S. Nishiwaki, L. Weinhardt, S. Pookpanratana, O. Fuchs, M. Blum, W. Yang, J. D. Denlinger, W. N. Shafarman, and C. Heske, Appl. Phys. Lett. **93**, 244103 (2008).

[59] R. Klenk, Thin Solid Films **387**, 135 (2001).

[60] R. J. Matson, J. E. Granata, S. E. Asher, and M. R. Young, *Proc. 15th NCPV Photovoltaic Program Review*, Denver, CO, 1998 (AIP, Melville, NY, 1999), Vol. **462**, 542.

[61] A. Rockett, J. S. Britt, T. Gillespie, C. Marshall, M. M. Al Jassim, F. Hasoon, R. Matson, and B. Basol, Thin Solid Films **372**, 212 (2000).